



The next generation radiotelescopes / Les radiotélescopes du futur

## Antenna design and distribution of the LOFAR super station

### *Conception et distribution d'antennes pour une super station LOFAR à Nançay*

Julien N. Girard<sup>a,\*</sup>, Philippe Zarka<sup>a</sup>, Michel Tagger<sup>b</sup>, Laurent Denis<sup>c</sup>, Didier Charrier<sup>d</sup>, Alexander A. Konovalenko<sup>e</sup>, Frédéric Boone<sup>f</sup>

<sup>a</sup> Laboratoire d'études spatiales et d'instrumentation en astrophysique (LESIA), observatoire de Paris, CNRS, UPMC, université Paris-Diderot, 5, place Jules-Janssen, 92190 Meudon, France

<sup>b</sup> Laboratoire de physique et chimie de l'environnement et de l'espace (LPC2E), université d'Orléans, 3A, avenue de la recherche scientifique, 45071 Orléans cedex 2, France

<sup>c</sup> Station de radioastronomie, observatoire de Paris, CNRS, route de Souesmes, 18330 Nançay, France

<sup>d</sup> Laboratoire de physique subatomique et des technologies associées (SUBATECH), École des mines de Nantes, CNRS/IN2P3, université de Nantes, 4, rue Alfred-Kastler, La Chantrerie BP 20722, 44307 Nantes cedex 3, France

<sup>e</sup> Institute of Radio Astronomy (IRA), National Academy of Sciences, 4, Krasnoznamenaya St., 61002 Kharkov, Ukraine

<sup>f</sup> Institut de recherche en astrophysique et planétologie (IRAP), université Paul-Sabatier, CNRS, 9, avenue du Colonel Roche, BP 44346, 31028 Toulouse cedex 4, France

#### ARTICLE INFO

##### Article history:

Available online 11 December 2011

##### Keywords:

Antennas  
Phased array  
Interferometer  
Configurations  
LOFAR

##### Mots-clés:

Antennes  
Réseaux phasés  
Interféromètre  
Configurations  
LOFAR

#### ABSTRACT

The Nançay radio astronomy observatory and associated laboratories are developing the concept of a “Super Station” for extending the LOFAR station now installed and operational in Nançay. The LOFAR Super Station (LSS) will increase the number of high sensitivity long baselines, provide short baselines, act as an alternate core, and be a large standalone instrument. It will operate in the low frequency band of LOFAR (15–80 MHz) and extend this range to lower frequencies. Three key developments for the LSS are described here: (i) the design of a specific antenna, and the distribution of such antennas; (ii) at small-scale (analog-phased mini-array); and (iii) at large-scale (the whole LSS).

© 2011 Académie des sciences. Published by Elsevier Masson SAS. All rights reserved.

#### RÉSUMÉ

L'Observatoire de Nançay et des laboratoires associés développent un concept de “Super Station” afin d'étendre les capacités de l'actuelle station LOFAR installée à Nançay. La Super Station LOFAR (LSS) augmentera le nombre de longues bases interférométriques sensibles, fournira de nouvelles bases courtes, formera un cœur alternatif à LOFAR et constituera un nouvel instrument autonome. Il opérera dans la bande basse de LOFAR (15–80 MHz) et étendra cette bande à plus basses fréquences. Trois études clefs sont décrites ici: (i) La conception d'antennes spécifiques, et leur distribution; (ii) à petite échelle (dans un mini-réseau phasé analogique); et (iii) à grande échelle (réseau LSS).

© 2011 Académie des sciences. Published by Elsevier Masson SAS. All rights reserved.

\* Corresponding author.

E-mail addresses: [julien.girard@obspm.fr](mailto:julien.girard@obspm.fr) (J.N. Girard), [philippe.zarka@obspm.fr](mailto:philippe.zarka@obspm.fr) (P. Zarka), [michel.tagger@cnrs-orleans.fr](mailto:michel.tagger@cnrs-orleans.fr) (M. Tagger), [laurent.denis@obs-nancay.fr](mailto:laurent.denis@obs-nancay.fr) (L. Denis), [didier.charrier@subatech.in2p3.fr](mailto:didier.charrier@subatech.in2p3.fr) (D. Charrier), [akonov@ri.kharkov.ua](mailto:akonov@ri.kharkov.ua) (A.A. Konovalenko), [frederic.boone@irap.omp.eu](mailto:frederic.boone@irap.omp.eu) (F. Boone).

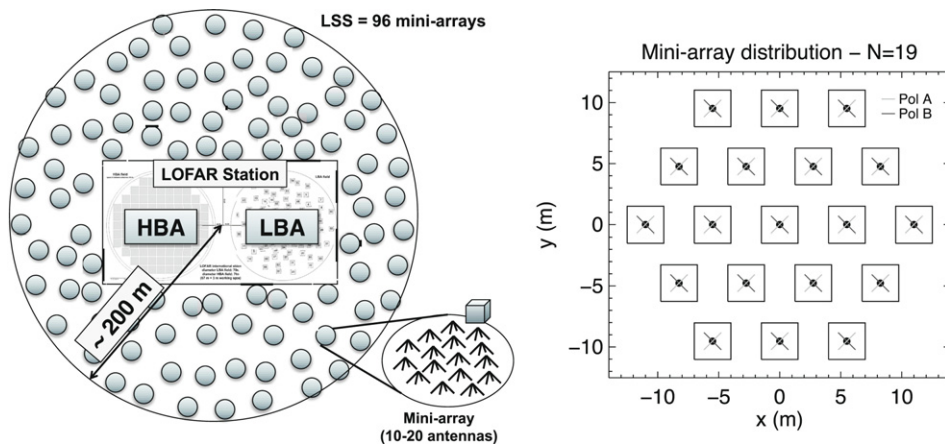


**Fig. 1.** Left: The LSS is a set of 96 mini-arrays of 10–20 analog-phased antennas, spread around the Nançay international LOFAR Station within a range of  $\sim 200$  m. Right: Possible antennas distribution within a mini-array, here on an hexagonal grid of  $N = 19$  elements. This distribution is a good compromise between an axisymmetric distribution (ensuring a symmetric main beam and low sidelobe level) and a regular array (providing easy analog phasing, but also grating lobes) (see Section 3.2).

## 1. Introduction

The renewed international interest for low frequency radioastronomy has given birth to many ground-based projects. One of them is the Dutch–European Low Frequency ARray (LOFAR) [1,2], working in the 15–240 MHz range. It is a very large radio interferometer composed of phased arrays of antennas (so-called “stations”) spread out to 100 km from a central “core” in the Netherlands, with remote stations at up to  $\sim 1000$  km in nearby European countries (currently France, Germany, Sweden, UK). Each LOFAR station actually consists of two phased arrays of 48 (NL) or 96 (European) antennas: the low band antenna (LBA) array below the FM band ( $\sim 30$ –80 MHz) and the high band antenna (HBA) array above it (110–240 MHz). Along with an electronic cabinet (digital control, command, and receivers), they form a LOFAR “station”. After digitization, beamforming, and spectral channelization, the signals of all stations are sent through an optical fiber link to the central correlator in Groningen. The Nançay Radio Observatory ([www.obs-nancay.fr](http://www.obs-nancay.fr)) hosts the international station “FR606”.

## 2. The LOFAR super station

### 2.1. Principle and general design

At any given time, a LOFAR station can use the LBA or the HBA field of antennas (not both) which are thus connected to two different inputs to the back-end. A third input to the cabinet’s receivers exists and was initially dedicated to a “Low Band Low” antenna field in the range 10–50 MHz. It is currently used in Dutch stations to allow different LBA configurations but it is still unused in the international stations. The main idea underlying the LSS concept is to build and connect to this input on FR606 a new field of 96 antennas (the LSS field), operating in the LBA range and extending this range to lower frequencies (down to  $\sim 15$  MHz). Each of these new antennas consists of an analog-phased mini-array of 10–20 antennas, thus increasing the sensitivity of the station by a factor 10–20, while remaining fully compatible with the whole LOFAR array. Each mini-array is very similar in its principle to a HBA tile of 16 ( $4 \times 4$  square grid) high frequency antennas, thus forming “LSS tile”. LSS tiles also consist of dual-polarized crossed dipoles, phased using delay lines (commutable sets of coaxial cables inserting relative time delays between dipoles) so that their summed signals form a beam that can be pointed toward the direction of interest. The differences with HBA tiles include operation at lower frequencies, which implies larger antennas, and a mini-array layout, not necessarily regular. The signals beamformed at tile level are digitized and numerically combined in the cabinet’s back-end, either in summation (phased array) mode or in correlation (interferometer) mode. The LSS will consist of 96 mini-arrays distributed within  $\sim 200$  m of the LOFAR station cabinet (see Fig. 1, right). Its layout must then be optimized at two different scales: mini-array and full LSS.

### 2.2. Interests of the LOFAR super station

#### 2.2.1. Within the LOFAR array

The LSS will provide several improvements to the present LOFAR design and capabilities.

First, the  $\approx 10$ – $20\times$  improved sensitivity of the mini-array, compared to a standard LBA antenna, will correspondingly increase the sensitivity of the 47 long baselines involving the LSS. Moreover, the six closest LOFAR stations gathered in the core (called the “SuperTerp”) provide six almost identical baselines (therefore, six very close points for these baselines in the  $(u, v)$  plane of LOFAR, comparable to one “sensitive”  $(u, v)$  point) with each one of the 41 remaining stations. As a result,

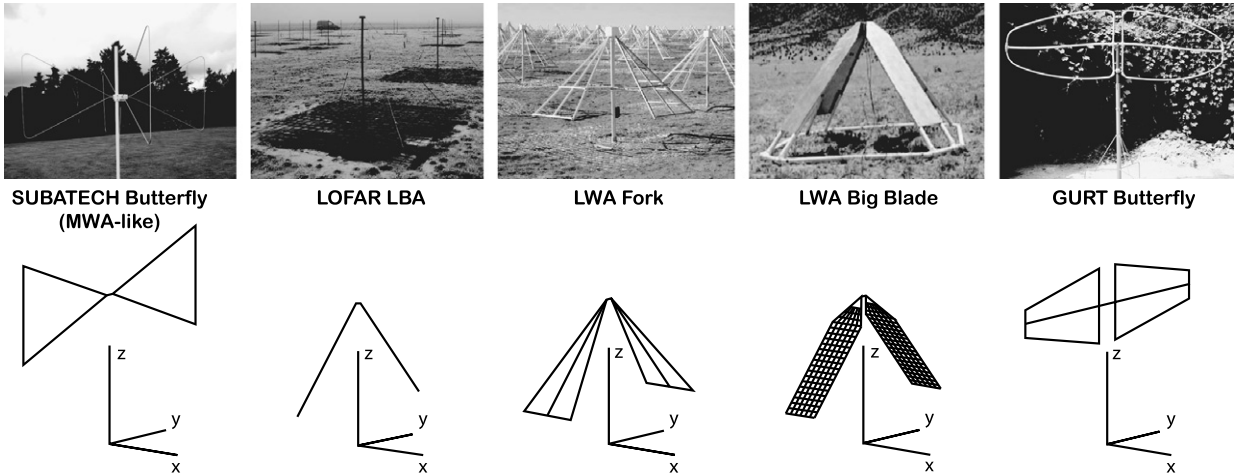


**Fig. 2.** The top panel displays the linearly polarized dipoles that have been studied in Nançay (from different ground-based projects: the Long Wavelength Array (LWA), LOFAR and the Giant Ukrainian RadioTelescope (GURT)). The bottom panel displays the numerical wire models used as input to electromagnetic simulations with NEC. Simulated beam patterns are shown in Fig. 3.

the SuperTerp and the eight international stations provide eight very long and very sensitive baselines. The LSS, by being far from all other stations, will thus approximately bring five times more very long baselines with very high sensitivity in the low band of LOFAR (or  $\approx 2.5$  times the total number of very long baselines in the two bands of LOFAR).

Second, only station-to-station correlations were planned in the initial LOFAR project. In the LBA range the minimum baseline length is the LBA field diameter ( $B_{\min} \sim 60$  m). This implies that LOFAR would be blind to structures larger than  $\lambda/B_{\min}$  at wavelength  $\lambda$  (i.e. typically larger than a few degrees). It is planned to perform antenna-to-antenna correlations within LBA fields or within the SuperTerp, but the sensitivity of each LBA is very poor. With the LSS, tile-to-tile correlations will be performed, providing baselines as short as a mini-array diameter ( $\approx 20$  m) and up to the LSS diameter ( $\sim 400$  m) with 10–20 times better sensitivity. LSS will thus fill a missing part of LOFAR's present ( $u, v$ )-coverage in the low band.

Third, several LOFAR observation programs (e.g. "Epoch of Reionization") will need large bandwidths and excellent calibration rather than high angular resolution and will consequently use only core stations. In the meantime, remote and international stations may be correlated in parallel by the central computer and run other programs, but without the benefits (sensitivity and short baselines) of the core stations. By correlating the LSS to all remaining stations, sensitive long baselines will be restored. The LSS can thus be viewed as an alternate core forming an interferometer with decent ( $u, v$ )-coverage and good sensitivity, and running in parallel to programs requiring the core. In this way, the LSS can contribute to "create" up to 30% of additional LOFAR observing time in parallel with core-only observations ( $\approx 4000$  h during  $\approx 2$  years – see <http://www.astro.rug.nl/~lofareor> and references therein).

### 2.2.2. As a stand-alone instrument

With  $N = 19$  antennas (Fig. 1, right), the LSS will have an effective area  $\simeq 96 \times 19\lambda^2/4 = 456 \times \lambda^2/4$ ,  $\simeq 3 \times$  the Very Large Array (VLA) in New-Mexico at 73.8 MHz or  $\simeq 20 \times$  the Nançay Decameter Array (NDA) at 20 MHz ([3] and references therein). It will thus be a large instrument by itself, with relevant standalone use independent of LOFAR, with no loss for LOFAR when the Nançay FR606 station is not included in ongoing observations (this should represent at least 10% of the time for international stations). Moreover, the LSS antennas can be designed in order to provide a better sensitivity (with an improved antenna design and enhanced preamplifiers) and immunity to radio frequency interference (RFI) than LBAs, and to extend the spectral range of operation down to frequencies below 30 MHz.

## 3. Three key design studies for the LSS

### 3.1. Antenna design

Antenna design implies the determination of physical (geometrical) and electrical parameters of the antenna radiators, which will in turn constrain the performance of the array in which they are grouped. For different existing projects (as shown in Fig. 2), antennas have been developed in order to meet specific scientific and technical requirements. These parameters are the antenna beam pattern E- and H-planes (constraining the array's Field of View – FoV (see Fig. 3)), the frequency bandwidth and the efficiency (related to electrical and ground losses). At low frequencies, the antennas are in a sky noise dominated regime ( $T_{\text{sky}} \approx 60,000$  K at 20 MHz  $\gg T_{\text{inst}}$ , the instrumental noise component), therefore any consideration about reducing the system temperature is not necessary. The performance of different low noise amplifiers (LNA), are currently tested in Nançay.

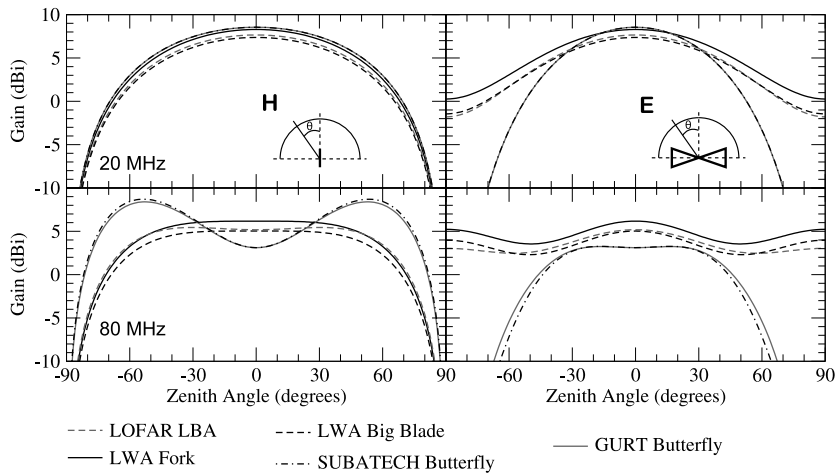


**Fig. 3.** Directional gain of the antenna models of Fig. 2 in dBi (an ideal isotropic antenna at 0 dBi is the reference) as a function of the zenith angle  $\theta$ . The two principal planes (H plane and E plane) are shown for two characteristic frequencies of the LSS. Antenna geometries were adjusted to a common scale so as to facilitate comparisons (strand length and height are 1.5 m). The ground is assumed to be perfectly conductive. From these plots, the LWA Fork antenna (thick black line) provides smooth pattern characteristics over the band 20–80 MHz (see Section 3.1). We also studied the influence of all geometrical parameters, the presence of a realistic lossy ground and the addition of a ground screen under the antenna, on the antenna characteristics (pattern, radiation efficiency, input impedance variation, etc.).

For a phased array application such as the LSS, a large and smooth beam pattern (with little gain ripples) is required, close to that of an isotropic antenna, as it will determine the final scan range of the array, which is expected to go down to an elevation of  $20^\circ$  with LOFAR. Toward the horizon, extinction of the beam is preferred to reduce the susceptibility to RFIs. We also wish to obtain a broadband antenna that can operate down to 10–20 MHz, implying an antenna input impedance as constant as possible over the band of interest.

We restrained studies to linearly polarized dipoles, since circularly polarized antennas such as those of the NDA [4] are quite expensive. Using the Numerical Electromagnetic Code (NEC – [www.nec2.org](http://www.nec2.org)), we compared different geometries and surroundings of the radiators. This method of moments code can derive the simulated far field pattern and the electrical parameters of any antenna defined by a wire model (see bottom panel of Fig. 2) and feed. We investigated two classes of radiator designs (“butterfly” (derived from biconical antenna [5]) and “inverted-V” antennas) and the influence of a ground plane (metal grid) over a perfect or a realistic lossy ground and we performed optimization studies of their parameters (height, length, droop and apex angles, grid mesh size and step, etc.).

From Fig. 3, showing the results of simulations in an ideal scenario (perfectly conductive ground, same feed, no loss, scaled models), the two butterfly designs do not satisfy our objective of having a large FOV over the LSS band in the two principal planes of the antennas : a gain decrease develops at zenith ( $-6$  dB relatively to the maximum gain at 80 MHz, due to the height of the antenna as compared to  $\frac{\lambda}{4}$ ) and the beam width in the E-plane is quite low ( $\approx 80^\circ$  at  $-3$  dB) as compared with other models. The inverted-V antennas, because of their geometry, are less subject to this effect, but are quite sensitive to emission coming from horizon (e.g. RFIs).

These studies led us to select a “thick” [5] inverted-V dipole similar to the LWA Fork, which appeared to be a good compromise between bandwidth, FoV and gain. We found that – as for LOFAR and the LWA – a metallic ground screen is necessary for inverted-V antennas in order to reduce ground losses (efficiency  $>50\%$  at 20 MHz and  $>80\%$  at 80 MHz of that of a perfect plane), and to ensure the stability of the antenna impedance against variations of ground characteristics (dry or wet ground). In parallel, various LNA architectures and matching have been considered. A first prototype of this thick dipole has been built in Nançay.

### 3.2. Distribution of antennas within a mini-array

The role of the mini-array is to combine analog antenna signals to synthesize a single wide beam and coarsely point it in the sky. The fine pointing of the LSS beam (combination of the 96 signals tapered by the mini-array and the antenna beam patterns) will be performed by the beamforming system in the station back-end.

This beamformer is based on the narrowband assumption whose limits are detailed in [6]. In the case of the LSS, the decorrelation loss (function of the signal bandwidth, the size of the array and the signal incoming direction), may be as high as 11% at  $20^\circ$  elevation. The science case constraints on the distribution of the antennas within a mini-array include : a large effective area (high sensitivity), a smooth primary beam with a low level of side lobes, a not too complex phasing scheme, a low mutual coupling between antennas, etc. The distance between antennas is a result of a compromise between effective area overlapping and the frequency of appearance of grating lobes (in a regular mini-array).

We first performed an optimization study of the mini-array distribution by using simulated annealing [7] aiming at the maximum reduction of the sidelobes level (by taking the “energy” in sidelobes as a cost function). The resulting distributions are dense arrays (with a minimal inter-antenna distance) displaying circular symmetries around the phase center but without signs of periodicity (no superimposition to itself by any rotation  $\neq 2\pi$ ). Such an axisymmetric and aperiodic shape bring the minimization of the side lobes around the primary beam (down to  $-30$  dB attenuation or more) and the absence of strong grating lobes. But the irregularity of such arrays imposes a more complex phasing scheme (one full delay line per antenna).

Thus, we opted for an array of antennas presenting regularities along two orthogonal  $x$  and  $y$  directions (as in NDA or GURT), while being as close as possible to the optimized symmetric solutions found above. Regularities along  $x$  and  $y$  directions allow us to decompose the phasing scheme in two successive steps (e.g. phasing of antenna lines along  $x$  followed by phasing of rows along  $y$ ). The smart combinations of symmetrical antenna pairs relative to the center of each line allow quite large cable savings. A good compromise between beam characteristics and phasing complexity is shown in Fig. 1. Regular arrays simplify the handling of mutual coupling between antennas, because all embedded antennas (i.e. not at the edges of the mini-array) behave in a similar way. Conversely, in irregular/aperiodic arrays, the coupling may vary substantially from one antenna to the next, modifying antenna beam shapes, so that the synthesized mini-array beam may differ from the theory. Further studies of distribution, phasing, and coupling effects are ongoing.

### 3.3. Distribution of mini-arrays within the LSS

The LSS will consist of 96 mini-arrays distributed in an area of  $\sim 400$  m diameter (fixed by cable losses and terrain constraints) around the back-end of the FR606 station. It will work either in a phased-array (also called “tied-array beam” or “single pixel”) mode, as any standard station, or in interferometer mode. The digitization of each mini-array output (beamformed) signal by the LOFAR station back-end gives a large flexibility in the distribution of the 96 mini-arrays. The main constraints that the LSS must fulfill are a low side lobe level (in phased array mode) and a “good”  $(u, v)$  coverage by the  $96 \times 95/2$  baselines (in interferometer mode). As the filling factor of a disk of 400 m diameter by mini-arrays of 19 antennas is high ( $\sim 60\%$  at 20 MHz), the LSS will be a rather dense array/interferometer at low frequencies. We used another optimization algorithm described in [8]. It is a “pressure-driven” algorithm that enables to optimize the  $(u, v)$ -coverage (relative to a target Gaussian  $(u, v)$ -model) of a “gas” of individual antennas, taking into account an input “site mask” (accounting for local constraints: pond, buildings, other instruments, etc.). To taper the grating lobes introduced by the mini-array triangular lattice, each mini-array is relatively rotated by a random angle but all antennas are kept parallel in order to maintain the two main polarization axes between mini-arrays, as was done between LOFAR antenna fields of different stations. We computed that this decreases the side lobes level by  $\sim 8$  dB. This rotation also modifies the mutual coupling between antennas within each mini-array (as the antennas are oriented differently relative to the mini-array layout). Each mini-array will therefore have a different response, which complexifies dramatically the classical calibration methods. We are currently modeling the LSS measurement equation (defined by Jones matrices describing all effects affecting the signal path) using the MeqTrees package [9].

## 4. Conclusion

LSS detailed design, prototype and test studies (including the construction of 3 mini-arrays), and cost evaluation, will be pursued in the next  $\sim 20$  months. Its detailed scientific case is being developed in parallel. We expect LSS construction to start in 2013. If the concept is successful, it could be applied by other European participants to LOFAR, preparing a future “super LOFAR”.

## Acknowledgements

The authors acknowledge the support of the Observatoire de Paris, the CNRS/INSU, and the ANR (French “Agence nationale de la recherche”) via the program NT09-635931 “Study and Prototyping of a Super Station for LOFAR in Nançay”. The authors acknowledge S. J. Wijnholds for his useful comments and suggestions which helped to improve the clarity of the paper.

## References

- [1] J.-M. Grießmeier, P. Zarka, M. Tagger, Radioastronomy with LOFAR, C. R. Physique 13 (1) (2012) 23–27, in this issue.
- [2] M. De Vos, A.W. Gunst, R. Nijboer, The LOFAR telescope: System architecture and signal processing, Proc. IEEE 97 (8) (2009) 1431–1437.
- [3] J.-M. Grießmeier, P. Zarka, J.N. Girard, Observation of planetary radio emissions using large arrays, Radio Sci., in press, doi:10.1029/2011RS004752.
- [4] A. Boisshot, et al., A new high gain, broadband, steerable array to study jovian decametric emission, Icarus 43 (1980) 399–407.
- [5] C.A. Balanis, Antenna Theory: Analysis and Design, 2nd ed., Wiley, 2005, pp. 497–522.
- [6] S.J. Wijnholds, Fish-Eye Observing with Phased Array Radio Telescopes, Technische Universiteit Delft, PhD Thesis, 2010. ISBN 978-90-9025180-6.
- [7] S. Kirkpatrick, C.D. Gelatt, M.P. Vecchi, Optimization by simulated annealing, Science New Series 220 (4598) (1983) 671–680.
- [8] F. Boone, Interferometric array design: Optimizing the locations of the antenna pads, Astron. Astrophys. 377 (2001) 368–376.
- [9] J.E. Noordam, O.M. Smirnov, The MeqTrees software system and its use for third-generation calibration of radio interferometers, Astron. Astrophys. 524 (2010) A61.